DINAME 2023 - Proceedings of the XIX International Symposium on Dynamic Problems of Mechanics,
A.S. De Paula, A.T. Fabro and M.R. Machado (Editors), ABCM.
Pirenópolis, Go, Brazil, February 26th to March 3rd, 2023

Comparison of passive dynamic absorbers in attenuating pathological tremor of human upper limb: an analytical approach

G.G.deS.B.de Albuquerque, B.B. de Moura, M.R. Machado

Department of Mechanical Engineering, University of Brasília, 70910-900, Brasília, Brazil.

Abstract: Tremors in the human body are characterised by a rhythmic oscillation of the limb that can cause social discomfort and difficulty performing basic everyday tasks. Some physiological conditions or neuro-degenerative diseases, such as Parkinson's disease, often cause tremors in the wearer's limbs. This tremor is often associated with social discomfort and difficulties performing certain movements. This work aims to analyse the efficiency of passive vibration control in a human upper limb of a patient with Parkinson's disease under two excitation levels. Analytical models of the arm and passive controls are used to estimate the arm's vibration characteristic and investigate the control's efficiency under two levels of pathology tremor excitation.

Keywords: Tremor, Parkinson Disease, Dynamic absorber

INTRODUCTION

Tremors in the human body are characterised by a rhythmic oscillation of the limb that can cause social discomfort and difficulty performing basic everyday tasks. Although limb tremor is easy to notice in some cases, diagnosis requires careful investigation as several conditions present with this symptom, and treatments can vary considerably from one disease to another as presented in (Crawford III and Zimmerman, 2018). In human limbs is an increasingly present need in individuals with neurodegenerative diseases such as Parkinson's Disease, White Hand Syndrome, Essential Tremor, Induced Tremor and others (Chou, 2004). Generally, these diseases have a series of unpleasant symptoms. Also, there are some medications that can cause symptoms similar to those of Parkinsonism.

One of the most prominent is tremors in the upper limbs, occurring more frequently in the individual's fingers, hands and arms. In the context of Parkinson's diseases, tremors are defined by repetitive and involuntary oscillations in the limbs which usually initiates in upper limbs. They may occur, in a lasting way, in postural conditions (limb in a resting or static position), kinetic (limb in movement) or both (Crawford III and Zimmerman, 2018). The rest tremor of Parkinsonism is in the range between 3 and 7 Hz, whereas the postural tremor is in the range between 5 and 12 Hz as shown in Morrison *et al.* (2008). In addition, tremors can also be classified by frequency (high, intermediate and low) and amplitude of oscillations (coarse, medium and fine).

Some alternatives to treat those neurodegenerative diseases or to control the corresponding tremors are already being explored through drugs, surgery, electrical stimulation, light therapy, transcranial magnetic stimulation, orthoses and vibration attenuating devices. However, each alternative may present negative or impeding points, varying from individual to individual (Diaz and Louis, 2010). Thus, when considering the possibility of drug allergy, the degree of invasion of the treatment and the efficiency of the treatment, it is inevitable the use of vibration attenuating devices stand out from the others in combating tremors in the limbs (Fromme *et al.*, 2019).

To reduce the burden of this disease, a dynamic vibration absorber can be designed to suppress the undesirable motion. The dynamic vibration absorber (DVA) is a passive vibration controller added in a system to as part of a remedial course of action at a particular frequency. The parameters of it are chosen to minimize the amplitude, principally the vibration at an undesired frequency. The limb system behavior can be translated into the movements of masses. Hashemi *et al.* (2004) proposed a two degree-of-freedom (DOF) model of upper limb with mass concentrated at centroid and inertia. The human arm was shaped on the horizontal plane as two rigid segments to describe the arm musculature planar motion of elbow and shoulder joints, but motion at wrist joint was not included. Gebai *et al.* (2016a) improved the mass-spring model considering the human hand as a three DOF system by increasing the motion of the palm. Also, he added the motion transmitted to the palm and the wrist joint as well as the movements from the biceps.

In this paper, we compare the efficiency of different configurations of single and dual passive dynamic absorber controllers in minimizing vibration originated from an excitation of human upper limb structure by Parkinson's disease. The analytical models of the arm and passive controls approached in this paper follow the work of Gebai *et al.* (2018), and study of the limber under two levels of pathology tremor excitation is performed. Results show the efficiency of the dynamic absorbers that could drastically attenuate the tremor.

HUMAN UPPER LIMB STRUCTURE

The analytical model of the upper limb used in the study follows the model presented by Gebai *et al.* (2016a) and Hosseini *et al.* (2021). It consists of three-degree-of-freedom biodynamic modelling that considers the flexion-extension planar motion in the horizontal plane at the shoulder, elbow and wrist joints. Figure 1(LHS) shows the human upper limb parts and Fig. 1(RHS) the model proposed by the authors. The active input moments producing motion are considered due to the shoulder and elbow muscle activation operating at the problematic frequencies in the range of the resting tremor.

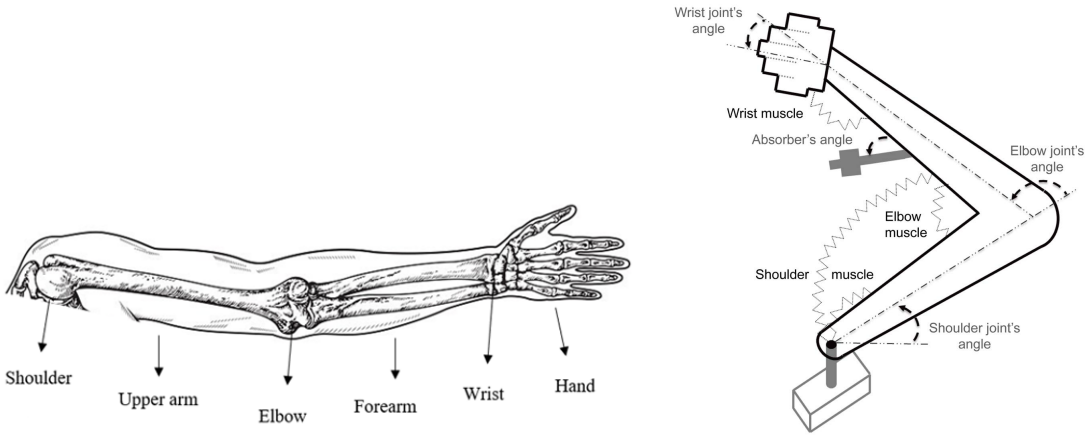

Figure 1: Schematic of a Human upper limb (LHS) and relation of the bio-mechanical model (RHS) by Gebai *et al.* (2018)

Mechanical upper limb design

The parameters of mass and inertia, as well as the length, mass, density and position of the centroid for the right hand, were calculated based on data provided experimentally by Contini (1972). The length of upper arm is represented by l_1, forearm by l_2, and palm by l_4, as shown in Fig. 2, and Table 1 contain the mass and inertia of each segment. The total mass of the considered system is 3.77 kg. The centroids are refereed in Fig. 2 as a_1 (upper arm), a_2 (forearm) and a_4 (palm), and inertia of the upper arm by I_1, the forearm by I_2, and the palm by I_4. Three configurations of dynamic vibration absorbers (DVA) are tested and settled at point B on l_a position from point A (elbow), as shown in Fig. 2. The position from the absorber's mass to its joint along the beam is a_3 for the SA1 configuration and a_5 for SA2. In point 3, the absorbers are considered with an additional mass of m_d=52.2 g to increase the controller device (Gebai *et al.*, 2016a). When the single absorbers are attached individually, l_3 is equal to l_a. In the DPA, there are two devices, so the total device mass is 104.4 g.

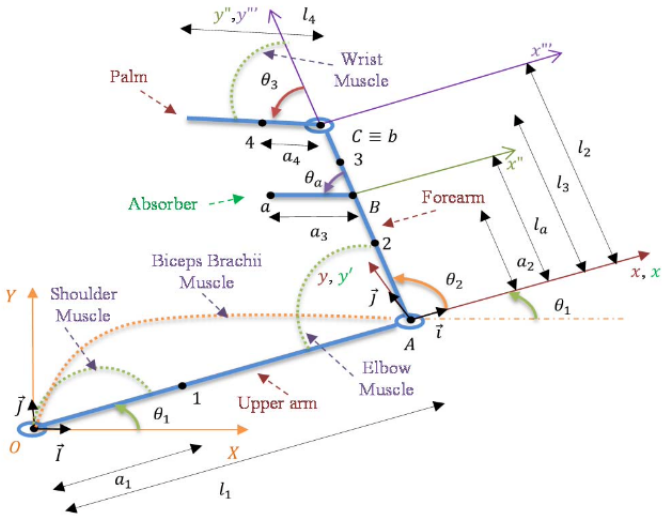

Figure 2: Controlled hand modeled system (Gebai *et al.*, 2016a).

Table 1: Hand Arm Parameters (Gebai *et al.*, 2016a)

Right Hand	Length (cm)	Mass (kg)	Density (kg/m^3)	Centroid (m)	Moments of Inertia (kgm^2/rd)
Upper arm	36.4	2.070	1088.0	$0.427 \cdot l_1$	0.0228
Forearm	29.9	1.160	1108.6	$0.417 \cdot l_2$	0.0082
Palm	20.3	0.540	1112.6	$0.361 \cdot l_4$	0.0012

Table 2 lists the stiffness values assumed at the shoulder's joint indicated by k_1, elbow as k_2, biceps as k_3, and wrist as k_4.

Table 2: Designed Parameters of Joint's Muscles (Gebai *et al.*, 2016a)

Muscle	Stiffness coefficient ($N \cdot m/rd$)	Damping coefficient ($N \cdot m \cdot s/rd$)
Shoulder	170	$0.002 \cdot k_1$
Elbow	150	$0.002 \cdot k_2$
Biceps	40	$0.002 \cdot k_3$
Wrist	10	$0.001 \cdot k_4$

DYNAMIC MODEL OF THE UPPER LIMB

The dynamic model of the upper limb, named the principal system, consists of a three-DOF system. The motion will start at an instance of stability when $\theta_1 = 0^o$, $\theta_2 = 90^o$, and $\theta_a = 0^o$ with zero angular velocities as indicated in Fig. 2. The equation of motion follows Gebai *et al.* (2016c). The kinematics equations used Coriolis Theorem to obtain the three-DOF systems related to three angular displacements accroding to the global coordinate system, yields

$$v_1 = v_O + \Omega_{xyz/XYZ} \times r_{1/O} = a_1 \dot{\theta}_1 \, j \tag{1}$$

$$v_A = v_O + \Omega_{xyz/XYZ} \times r_{A/O} = l_1 \dot{\theta}_1 \, j \tag{2}$$

$$v_2 = v_A + (v_{2/A}) + \Omega_{xyz/XYZ} \times r_{2/A} = -a_2(\dot{\theta}_1 + \dot{\theta}_2) \, i + l_1 \dot{\theta}_1 \, j \tag{3}$$

$$v_C = v_A + (v_{C/A}) + \Omega_{xyz/XYZ} \times r_{C/A} = -l_2(\dot{\theta}_1 + \dot{\theta}_2) \, i + l_1 \dot{\theta}_1 \, j \tag{4}$$

$$v_4 = v_C + (v_{4/C})_{x'y'z'} + \Omega_{x'y'z'/XYZ} \times r_{4/C} = -[(a_4 + l_2)(\dot{\theta}_1 + \dot{\theta}_2) + a_4 \dot{\theta}_3] \, i + l_1 \dot{\theta}_1 \, j \tag{5}$$

Therefore, using the Lagrange equation, where the Rayleigh dissipation function is added to obtain the damping contribution, to form equations of motion for the systems will be

$$\frac{d}{dt}\left(\frac{\partial T}{\partial \dot{q}_i} - \frac{\partial U}{\partial \dot{q}_i}\right) - \frac{\partial T}{\partial q_i} + \frac{\partial U}{\partial q_i} = F_i + F_{ci} \, , \qquad i = \{1,2,3\} \tag{6}$$

The Kinetic Energy is represented as

$$T = [\frac{1}{2} I_1 \dot{\theta}_1^2 + \frac{1}{2} m_1 v_1^2] + [\frac{1}{2} I_2 (\dot{\theta}_1 + \dot{\theta}_2)^2 + \frac{1}{2} m_1 v_1^2] + [\frac{1}{2} I_4 \dot{\theta}_3^2 + \frac{1}{2} m_4 v_4^2] \tag{7}$$

where each segment (upper arm, forearm and palm) was representing your portion in motion. The Potential Energy is of the form

$$U = \frac{1}{2} k_1 \theta_1^2 + \frac{1}{2} k_2 \theta_2^2 + \frac{1}{2} k_3 (\theta_1 + \theta_2)^2 + \frac{1}{2} k_4 \theta_3^2 \tag{8}$$

and Rayleigh dissipation function is represented by

$$C = \frac{1}{2} c_1 \dot{\theta}_1^2 + \frac{1}{2} c_2 \dot{\theta}_2^2 + \frac{1}{2} c_3 (\dot{\theta}_1 + \dot{\theta}_2)^2 + \frac{1}{2} c_4 \dot{\theta}_3^2 \tag{9}$$

The generalized equation of motion has the form

$$\mathbf{M}\ddot{\theta} + \mathbf{C}\dot{\theta} + \mathbf{K}\theta = \mathbf{f} \tag{10}$$

where θ,$\dot{\theta}$, $\ddot{\theta}$ are the angular displacement, velocity and acceleration vectors at the hand joints, respectively. For the uncontrolled hand system, $\theta_{1,2,3}$ corresponds to the flexion angle at the shoulder, elbow and wrist joints, respectively. Hence, matrices are expressed as

$$\mathbf{M} = \begin{bmatrix} M_{11} & M_{12} & M_{13} \\ M_{21} & M_{22} & M_{23} \\ M_{31} & M_{32} & M_{33} \end{bmatrix} \tag{11}$$

where,

$$
\begin{aligned}
M_{11} &= (I_1 + m_1 a_1^2) + (I_2 + m_2 a_2^2) + m_2 l_1^2 + m_4 (l_1^2 + l_2^2 + a_4^2 + 2 l_2 a_4) \\
M_{12} &= (I_2 + m_2 a_2^2) + m_4 (l_2^2 + a_4^2 + 2 l_2 a_4) \\
M_{13} &= m_4 (a_4^2 + l_2 a_4) \\
M_{21} &= M_{12} \quad M_{22} = M_{12} \quad M_{23} = M_{13} \\
M_{31} &= M_{13} \quad M_{32} = M_{23} \quad M_{33} = I_4 + m_4 a_4^2
\end{aligned}
$$

$$
\mathbf{K} = \begin{bmatrix} k_1 + k_3 & k_3 & 0 \\ k_3 & k_2 + k_3 & 0 \\ 0 & 0 & k_4 \end{bmatrix} \tag{12}
$$

$$
\mathbf{C} = \begin{bmatrix} c_1 + c_3 & c_3 & 0 \\ c_3 & c_2 + c_3 & 0 \\ 0 & 0 & c_4 \end{bmatrix} \tag{13}
$$

Excitation force

The force $f_{1,2}$ are the input moments due to shoulder and elbow muscle activation, respectively. Those moments are driven at the first two resonance frequencies of the primary system as a dual harmonic function representing the resting tremor.

$$
\mathbf{f^T} = \begin{bmatrix} f1 & f2 & 0 & 0 \end{bmatrix}^T
$$

$$
\mathbf{f}_{1,2} = 1\cos(\omega_1 t) + 1\cos(\omega_2 t), \qquad \text{for} \quad \omega_1 = \omega_{n1}, \quad \text{and} \quad \omega_2 = \omega_{n2} \tag{14}
$$

where ω is the driving frequency of the muscles and ω_n is the natural frequency of the primary system.

Passive control systems

Gebai *et al.* (2018) proposed five different dynamics DVAs. In this paper, we investigated three absorbers inspired by his work. The DVAs are attached to the primary system aiming to control undesired vibration. The controllers are modelled as stainless steel alloy cantilevered beams with a copper mass attached with the same total mass of 206.8 g. The dual controllers it has two masses, each one weighing 103.4 g.

The first single absorber is tuned at the first natural frequency of the primary system, and the second absorber at the second natural frequency. The dual parallel conventional absorber (DPA) combines two similar devices (DVA). In this paper, the two singles absorbers (SA1 and SA2) are attached to the forearm at $l_{a_i} = 4\ cm$, where the l_{a_1} and the l_{a_2} assume similar values. However, the dual parallel absorber is attached to the forearm at $l_{a_1} = 9\ cm$ and $l_{a_2} = 4\ cm$ from the elbow. These values were chosen to potentialize the absorption of undesired vibration even more for working closely at the vibration source. Passive controls configurations attached to a primary system are Fig. 3 (a) single-degree-of-freedom absorber at the first natural frequency of the hand system (SA1), (b) single-degree-of-freedom absorber at the second natural frequency of the hand system (SA2), (c) dual parallel conventional tuned mass damper (DPA).

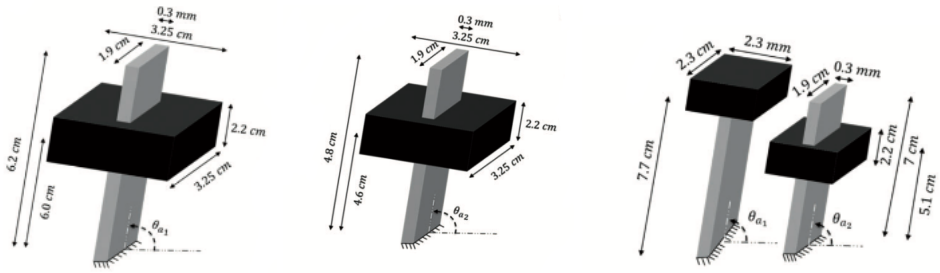

(a) (b) (c)

Figure 3: **Passive controllers modeled as cantilevered beam with attached proof mass: (a) SA1, (b) SA2 and (c) DPA (Gebai *et al.*, 2018).**

In this case, the equation of motion for the primary system within the controls follows the same steps as the primary

system. By using the SA1 on the primary system, the matrices yield

$$\mathbf{M} = \begin{bmatrix} M_{11} & M_{12} & M_{13} & M_{14} \\ M_{21} & M_{22} & M_{23} & M_{24} \\ M_{31} & M_{32} & M_{33} & M_{34} \\ M_{41} & M_{42} & M_{43} & M_{44} \end{bmatrix} \tag{15}$$

where

$$M_{11} = (I_1 + m_1 a_1^2) + (I_2 + m_2 a_2^2) + m_2 l_1^2 + m_4(l_1^2 + l_2^2 + a_4^2 + 2l_2 a_4) + m_{a_1}(l_1^2 + l_3^2) + m_{a_1}(l_1^2 + l_{a_1}^2 + a_3^2 + 2l_{a_1} a_3)$$

$$M_{12} = (I_2 + m_2 a_2^2) + m_4(l_2^2 + a_4^2 + 2l_2 a_4) + m_{a_1}(l_{a_1}^2 + a_3^2 + 2l_{a_1} a_3)$$

$$M_{13} = m_4(a_4^2 + l_2 a_4), \quad M_{14} = m_{a_1}(a_3^2 + l_{a_1} a_3)$$

$$M_{21} = M_{12} \quad M_{22} = M_{12} \quad M_{23} = M_{13} \quad M_{24} = M_{14}$$

$$M_{31} = M_{13} \quad M_{32} = M_{23} \quad M_{33} = I_4 + m_4 a_4^2 \quad M_{34} = 0$$

$$M_{41} = M_{14} \quad M_{42} = M_{24} \quad M_{43} = M_{34} \quad M_{44} = m_{a_1} a_3^2$$

$$\mathbf{K} = \begin{bmatrix} k_1 + k_3 & k_3 & 0 & 0 \\ k_3 & k_2 + k_3 & 0 & 0 \\ 0 & 0 & k_4 & 0 \\ 0 & 0 & 0 & k_{a_1} \end{bmatrix} \tag{16}$$

and

$$\mathbf{C} = \begin{bmatrix} c_1 + c_3 & c_3 & 0 & 0 \\ c_3 & c_2 + c_3 & 0 & 0 \\ 0 & 0 & c_4 & 0 \\ 0 & 0 & 0 & c_{a_1} \end{bmatrix} \tag{17}$$

Absorber design

The absorber design consist of a beam attached to a mass on the free tip as showing in Fig. 3 (Gebai *et al.*, 2016c). The dimension of each absorber is displayed on Table 3.

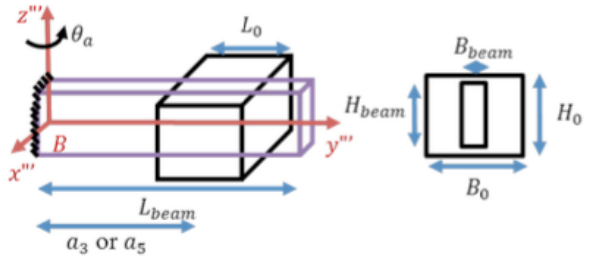

Figure 4: Designed dynamic vibration absorber (Gebai *et al.*, 2016c)

Table 3: Dimensions of the DPA system Gebai *et al.* (2018)

Absorber	Components	L (cm)	H (cm)	B (cm)
SA1	Beam	6.2	1.9	0.03
	Attached Mass	2.2	3.25	3.5
SA2	Beam	4.8	1.9	0.03
	Attached Mass	2.2	3.25	3.5
DPA-SA1	Beam	7.7	1.9	0.03
	Attached Mass	2.2	2.3	2.3
DPA-SA2	Beam	7	1.9	0.03
	Attached Mass	2.2	2.3	2.3

The position of the cooper mass in each absorber was calculated following The Dunkerley's semi-empirical formulation which gives a lower band approximation (Jeffcott, 1918) to satisfy the frequency tuning condition

$$\frac{1}{\omega_{a_i}^2} \simeq \frac{1}{\omega_{beam}^2} + \frac{1}{\omega_{m_0}^2}, \quad i = \{1,2\} \tag{18}$$

where

$$\omega_{beam} = 3.5160\sqrt{\frac{E_{beam}I_{beam}}{m_{beam}L_{beam}^3}} \tag{19}$$

$$\omega_{m_{a_i}} = \sqrt{\frac{6E_{beam}I_{beam}}{m_{a_i}a_i^2(3L_{beam}-a_i)}}\,, \quad i=\{1,2\} \tag{20}$$

by following (Gebai *et al.*, 2016c), the parameters are $E_{beam} = 189.6\ GPa$, $\rho_{beam} = 7800\ kg/m^3$, and $\rho_{m_{a_i}} = 8900\ kg/m^3$. Thus, the position of the proof mass in the SA1 and in The SA2, following the Table 3, respectively, are

$$a_3 \;=\; 6.02\ cm \quad and \quad a_5 \;=\; 4.60\ cm$$

In the DPA the positions assumed by each absorber are

$$a_3 \;=\; 7.66\ cm \quad and \quad a_5 \;=\; 5.08\ cm$$

The stiffness (k_{a_i}) and damping (c_{a_i}) coefficients are assumed to be proportional by a constant (Hashemi *et al.*, 2004), such that $c_{a_i} = 0.005\ k_{a_i}$, $i = \{1,2\}$, chosen to match the selected tuning frequency the system. The absorbers are designed to satisfy the loci frequency of $A_{1_{ij}}$. The dynamic response is obtained using the transfer function ($H(\omega) = \{(-\omega^2\mathbf{M}+\mathbf{K})+i\omega\mathbf{C}\}^{-1}$) of the coupled system. The frequency domain response (θ) is obtained using the receptance transfer function (α) as follows (Gebai *et al.*, 2016b)

$$\alpha_k = \begin{Bmatrix} \frac{A_{1_{ij}} + jB_{1_{ij}}}{A_2 + jB_2} \\ \cdot \\ \cdot \\ \cdot \\ \frac{A_{1_{nj}} + jB_{1_{nj}}}{A_2 + jB_2} \end{Bmatrix} = \begin{Bmatrix} \frac{\theta_{ij}}{F_j} \\ \cdot \\ \cdot \\ \cdot \\ \frac{\theta_{nj}}{F_j} \end{Bmatrix} \tag{21}$$

and the amplitude of angular displacement as

$$\theta_{ij} \;=\; \sum_{j=1}^{n} |\alpha_j| F_j \tag{22}$$

where i, j are the *i-th* row and *j-th* column for the $n \times n$ transfer function of the n-DOF system. Controllers tuned to the wrist joint's response due to shoulder muscle activation must satisfy the following condition $A_{1_{31}} = 0$ and $A_{1_{32}} = 0$. Hence, the stiffness of each absorber can be determined as shown in Table 4, in addition to the absorbers mass.

Table 4: The stiffness of absorbers

Works	SA1 (Nm/rd)	SA2 (Nm/rd)	DPA-SA1 (Nm/rd)	DPA-SA2 (Nm/rd)
Gebai *et al.* (2018)	0.3890	0.4918	0.3173	0.3009
In present work	0.3871	0.4917	0.3191	0.8174

Thereupon, we can simulate the respective absorbers from the parameters that satisfy the tuning conditions to evaluate their efficiency in tremor suppression.

RESULTS AND DISCUSSIONS

The natural frequency of each system mentioned in previews section is calculated by solving eigenvalue problems (Meirovitch, 2000). The results obtained in this work are close to the ones presented in Gebai *et al.* (2018). The natural frequency of each system is calculated by solving eigenvalue problems (Meirovitch, 2000), and the results are validated to the ones presented in Gebai *et al.* (2018). Table 5 gathers the frequencies for the hand and arm model without control and controlled by absorbers SA1, SA2, and DPA. All frequency values follow the refereed paper except for the DPA last frequency, which presents an error of 28%.

Table 5: The natural frequencies of hand arm model

Absorber	Reference	ω_{n1} (Hz)	ω_{n2} (Hz)	ω_{n3} (Hz)	ω_{n4} (Hz)	ω_{n5} (Hz)
No control	Gebai *et al.* (2018)	3.569	5.300	12.566		
	In present work	3.610	5.353	12.929		
SA1	Gebai *et al.* (2018)	3.194	3.891	5.435	14.822	
	In present work	3.260	3.649	5.096	12.855	
SA2	Gebai *et al.* (2018)	3.391	4.867	5.830	12.949	
	In present work	3.293	4.978	5.443	12.868	
DPA	Gebai *et al.* (2018)	3.227	3.813	4.995	5.686	12.890
	In present work	2.756	3.678	4.732	8.751	9.174

The position of each absorber in the forearm influences the tremor attenuation. In this paper, the distance placed SA1 and SA2 is l_a= 4 cm. On the other hand, in the DPA, the distance placed SA1 is l_{a_1} = 9 cm and SA2 is l_{a_2} = 4 cm. Gebai attached the majority of the absorbers at the same position on the forearm, which are far 8.5 cm from the wrist joint ($l_a = l_2$–$8.5cm$), decreasing the natural frequencies of the systems within DVAs.

Graphs of figures 5 and 6 show the system's behaviour in the frequency and time domains. A harmonic excitation expressed in Eg. (14) is input at the shoulder joint, where each excitation frequency correspond to the first limb natural frequencies. The results also demonstrate shoulder and elbow muscle activation dynamic response.

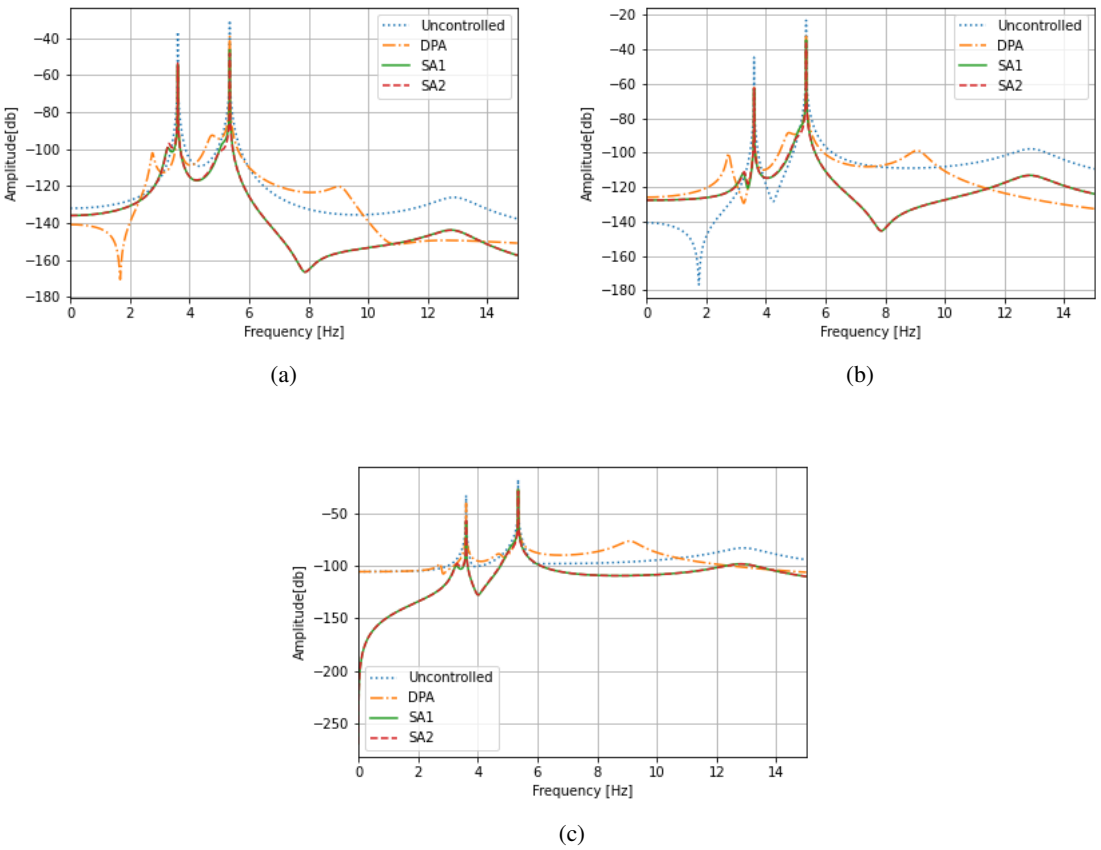

Figure 5: **Frequency domain response at the (a) shoulder joint, (b) elbow joint and (c) wrist joint.**

Figure 5a shows the frequency response function (FRF) obtained at the shoulder joint for the upper limb without control (blue dashed line) and controller using SA1 (green line), SA2 (red line), and DPA (orange line). The absorbers have designed values for each driving frequency to control the tremor. All absorbers can significantly reduce the resonant frequency magnitude, and the response from SA2 is similar to that from SA1. DPAs induced resonant frequencies in some bandwidths but presented a good control at the tuned frequency. It shows that the absorber can reduce the tremor's amplitude around the tuning frequency. Figures 5b and5c shows the FRF obtained at the elbow and wrist joints, with and

without control, respectively. A similar analysis applied to those two joints shows the controllers performing approximate attenuation of the shoulder.

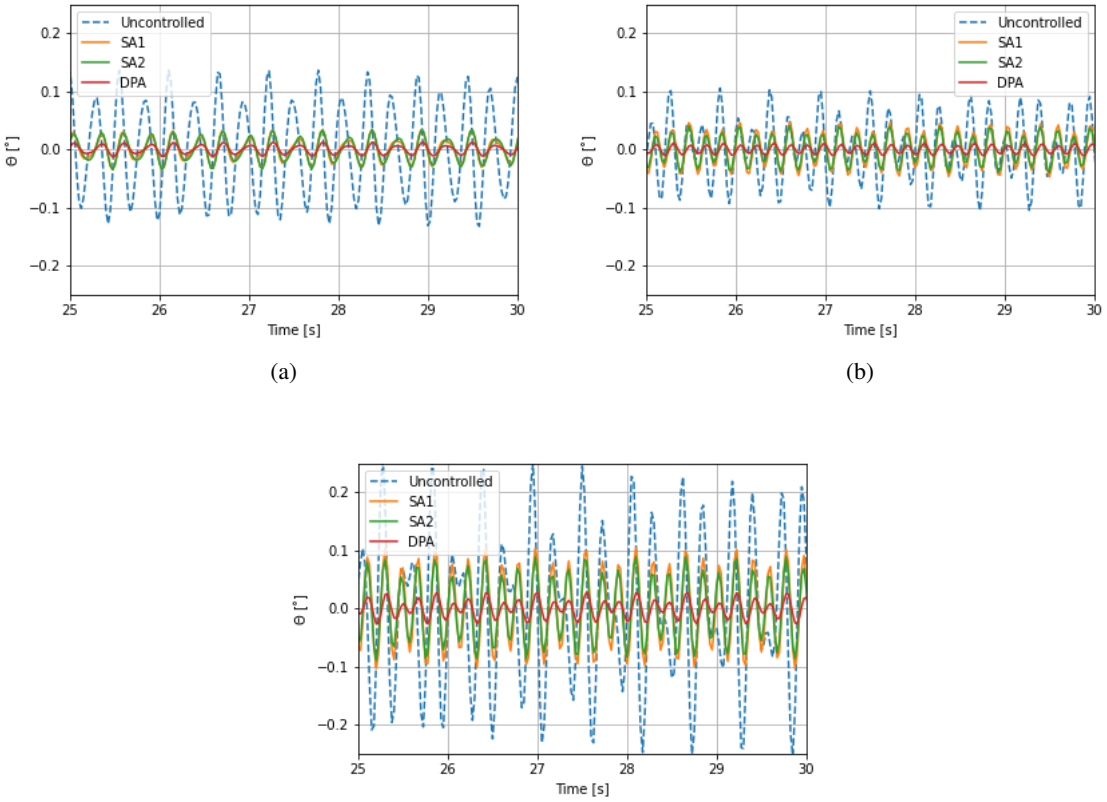

Figure 6: **Time domain response at the (a) shoulder joint, (b) elbow joint and (c) wrist joint.**

Figure 6 shows the temporal angular displacement for shoulder Fig. 6a, elbow Fig. 6b and wrist joints Fig. 6c. The highest reduction is provided by the system controlled by the dual parallel absorber (DPA) compared to the singles absorbers (SA1 and SA2). Furthermore, similar results were shown in Gebai's works. The DVAs have suppressed the amplitude of the primary system that can be estimated as the reduaction percentual calculated by (Gebai *et al.*, 2018)

$$Max.(\%\ Red.) = \frac{max.(\theta_{uncontrolled}) - max.(\theta_{controlled})}{max.(\theta_{uncontrolled})} \times 100 \tag{23}$$

The percental of amplitude reduction at the shoulder, elbow and wrist joints due to the single and dual controllers is presented in Table 6. All those results were calculated using the particular solution, given that the homogeneous response in range from 0 to 15 seconds, approximately.

Table 6: Percentage reduction in tremor's amplitude

Absorbers	Shoulder joint (%)	Elbow joint (%)	Wrist joint (%)
SA1	74.96	55.45	58.97
SA2	75.06	61.7	64.99
DPA	90.74	89.73	88.96

In comparison with Gebai *et al.* (2018), the singles absorbers are in the close range of percentage reduction. However, the DPA makes the highest reduction with this presetting configuration which can reduce the tremor to $90,74$ % at the shoulder joint, $89,73$ % at the elbow joint and $88,96$ % at the wrist joint. The DPA and SA2 were efficient controllers showing a good percentage reduction operating at a wide frequency band. Therefore, compared to uncontrolled ones, the controlled system shows a great decrease in amplitude in both time and frequency domain responses at the joints.

CONCLUSION AND FUTURE WORK

This paper intends to study and test the best configuration of absorbers in suppressing the tremor derived from Parkinson's patients. The responses of the uncontrolled and controlled structures are compared in the frequency and time domains. The efficiency of each controller was analyzed in terms of response magnitude and percentage of amplitude reduction. Indeed, the distance along the forearm measured from the elbow joint can significantly decrease the response amplitude if it is placed near the elbow joint. The best controller was the DPA amid those results with a large percentage reduction in the amplitude. The effect of more than two absorbers in parallel along the forearm can be analyzed after evidence of effectiveness in reducing the angular motion at the wrist joint. Hence, it can improve our knowledge of devices as well as guide us for new absorbers design applied to control human limb tremors.

ACKNOWLEDGMENTS

The author appreciate the supports from Fundação de Apoio a Pesquisa do Distrito Federal-FAPDF (Grants no. 00193-00000766/2021-71 and 00193- 00000826/2021-55)

REFERENCES

Chou, K.L., 2004. "Diagnosis and management of the patient with tremor". *Rhode Island Medical Journal*, Vol. 87, No. 5, p. 135.

Contini, R., 1972. "Body segment parameters, part ii". *Artificial limbs*, Vol. 16, No. 1, pp. 1–19.

Crawford III, P.F. and Zimmerman, E.E., 2018. "Tremor: sorting through the differential diagnosis". *American family physician*, Vol. 97, No. 3, pp. 180–186.

Diaz, N.L. and Louis, E.D., 2010. "Survey of medication usage patterns among essential tremor patients: movement disorder specialists vs. general neurologists". *Parkinsonism & related disorders*, Vol. 16, No. 9, pp. 604–607.

Fromme, N.P., Camenzind, M., Riener, R. and Rossi, R.M., 2019. "Need for mechanically and ergonomically enhanced tremor-suppression orthoses for the upper limb: a systematic review". *Journal of neuroengineering and rehabilitation*, Vol. 16, No. 1, pp. 1–15.

Gebai, S., Hammoud, M., Hallal, A., Al Shaer, A. and Khachfe, H., 2016a. "Passive vibration absorber for tremor in hand of parkinsonian patients: Tuned vibration absorber for rest tremor". In *2016 3rd International Conference on Advances in Computational Tools for Engineering Applications (ACTEA)*. pp. 162–167. doi:10.1109/ACTEA.2016.7560132.

Gebai, S., Hammoud, M. and Khachfe, H., 2016b. "Using a dual vibration absorber to suppress rest hand tremor of elderly". In *The Fifth International Conference on Global Health Challenges, GLOBAL HEALTH*.

Gebai, S., Hammoud, M., Hallal, A. and Al Shaer, A., 2018. "Structural control and biomechanical tremor suppression: Comparison between different types of passive absorber". *Journal of Vibration and Control*, Vol. 24, No. 12, pp. 2576–2590.

Gebai, S., Hammoud, M., Hallal, A. and Khachfe, H., 2016c. "Tremor reduction at the palm of a parkinson's patient using dynamic vibration absorber". *Bioengineering*, Vol. 3, No. 3, p. 18.

Hashemi, S., Golnaraghi, M. and Patla, A., 2004. "Tuned vibration absorber for suppression of rest tremor in parkinson's disease". *Medical and Biological Engineering and Computing*, Vol. 42, No. 1, pp. 61–70.

Hosseini, S.M., Kalhori, H. and Al-Jumaily, A., 2021. "Active vibration control in human forearm model using paired piezoelectric sensor and actuator". *Journal of Vibration and Control*, Vol. 27, No. 19-20, pp. 2231–2242.

Jeffcott, H., 1918. "The periods of lateral vibration of loaded shafts.—the rational derivation of dunkerley's empirical rule for determining whirling speeds". *Proceedings of the Royal Society of London. Series A, Containing Papers of a Mathematical and Physical Character*, Vol. 95, No. 666, pp. 106–115.

Meirovitch, L., 2000. "Fundamentals of vibrations/meirovitch, l".

Morrison, S., Kerr, G. and Silburn, P., 2008. "Bilateral tremor relations in parkinson's disease: Effects of mechanical coupling and medication". *Parkinsonism & related disorders*, Vol. 14, No. 4, pp. 298–308.

RESPONSIBILITY NOTICE

The author(s) is (are) the only responsible for the printed material included in this paper.